J. Biochem. **139**, 997–1005 (2006)
doi:10.1093/jb/mvj113

Comparison of Starch Hydrolysis Activity and Thermal Stability of Two *Bacillus licheniformis* α-Amylases and Insights into Engineering α-Amylase Variants Active under Acidic Conditions

Seunjae Lee[1], Hiroshi Oneda[1], Masashi Minoda[2], Akiyoshi Tanaka[3] and Kuniyo Inouye[1,*]

[1]Division of Food Science and Biotechnology, Graduate School of Agriculture, Kyoto University, Sakyo-ku, Kyoto 606-8502; [2]Daiwa Kasei Co., Konan-shi, Shiga 520-3203; and [3]Faculty of Bioresources, Mie University, Tsu, Mie 514-8507

Received December 23, 2005; accepted April 3, 2006

***Bacillus licheniformis* α-amylase (BLA) is widely used in various procedures of starch degradation in the food industry, and a BLA species with improved activity at higher temperature and under acidic conditions is desirable. Two BLA species, designated as PA and MA, have been isolated from the wild-type *B. licheniformis* strain and a mutant strain, respectively. In this study, their starch-hydrolysis activity and thermal stability were examined. MA showed higher activity than PA, especially at acidic pH (pH 5.0–5.5), and even after 1 h of treatment at 90°C. MA was active in the range of pH 4.0–8.0, which is much wider than that (pH 4.5–7.5) of PA. It was shown that the proton dissociation constants on the acidic and alkaline sides (pK_{a1} and pK_{a2}) were shifted to more acidic and basic values, respectively, by the mutation of PA to MA. The activation energy and thermodynamic parameters for their thermal inactivation indicate that MA is more thermally stable and catalytically active than PA, suggesting that MA could be useful for glucose-production process coupled with reactions catalyzed by β-amylase.**

Key words: α-amylase, *Bacillus licheniformis*, pH-dependence, starch hydrolysis, thermal stability.

Abbreviations: BLA, *Bacillus licheniformis* α-amylase; MA, mutant form of *B. licheniformis* α-amylase; PA, wild-type of *B. licheniformis* α-amylase.

α-Amylase specifically cleaves α-1,4–linked glucose polymers, thereby liquefying starch solution, decreasing its viscosity, decreasing its capacity to form blue color with iodine, and increasing the number of reducing ends of starch. α-Amylase is widely distributed in plants, animals, and microorganisms and shows various action patterns depending on the source. The enzyme has four regions of short amino-acid sequences that are conserved among species and make up the active site, which consists of three domains called A, B, and C (*1–4*). Domain A is a TIM-barrel [$(\alpha/\beta)_8$-barrel], which is interrupted by an irregular β-structure of domain B, inserted between the third β-strand and the third α-helix of the TIM-barrel. Domain C is a Greek key motif, which is located approximately on the opposite side of the TIM-barrel with respect to domain B. The reaction mechanism of *Bacillus licheniformis* α-amylase has been well defined (*5–8*). The active site is situated in a cleft at the interface between domains A and B, and consists of a large number of charged groups, among which three acidic amino acids (Asp 231, Glu 261, and Asp 328) are essential for the catalytic activity. Asp231 and Glu261 are the catalytic groups as a catalytic nucleophile and a catalytic hydrogen donor, respectively. Asp328 is believed to assist the catalysis by hydrogen bonding to the substrate and by elevating pK_a of Glu261.

α-Amylase is used in industrial processes in many ways (*9–11*). It is used for starch hydrolysis in starch liquefaction and in manufacturing fructose and glucose syrups; to improve flour in the baking industry; to produce modified starches for the paper industry; to remove starch in the manufacture of textiles (desizing); and as an additive to detergents for washing machines. Each of these processes takes place under physical and chemical conditions that are quite diverse. In the industrial production of glucose, starch-liquefaction by α-amylase and saccharifaction by β-amylase are carried out sequentially. Generally, α-amylase has an optimal pH of 7–8, while β-amylase has an optimum of pH 5–6, and the reactions must be performed at a temperature higher than 55°C to avoid bacterial contamination and to promote the reaction. In this process, adjusting the pH of the starch solution to optimize the two enzymatic reactions is troublesome, and selection of an appropriate enzyme pair of α- and β-amylases with enough thermal stability is a major problem remaining to be solved. From this viewpoint, changing the optimal pH of α-amylases to match that of β-amylase is desirable (*12*).

A thermostable α-amylase from *Bacillus licheniformis* IFO12196 strain (hereafter designated as PA or wild-type enzyme) has been widely used in liquefaction process. A mutant strain was isolated by treatment of the strain with *N*-methyl-*N*′-nitro-*N*-nitrosoguanidine (NTG) in Daiwa Kasei Co. (Shiga-ken, Japan), and a novel α-amylase (formerly named Y5, but herein designated as MA or

*To whom all correspondence should be addressed. Tel: +81-75-753-6266, Fax: +81-75-753-6265, E-mail: inouye@kais.kyoto-u.ac.jp

mutant enzyme) was identified from the mutant strain (*13*). It has been reported that PA has almost the same optimal pH (pH 7) as MA, but has an improved optimal temperature (95°C) in comparison with that (90°C) of PA (*13*). Because of this improved stability, MA has been considered more useful than PA for industrial processes of glucose production from starch.

In this study, we re-evaluate and compare the kinetic and thermodynamic aspects of the thermal stability and starch-hydrolyzing activity of PA and MA, and demonstrate that MA is more thermally stable and catalytically active in starch-liquefaction than PA, suggesting that MA could be useful for industrial production of glucose coupled with the β-amylase reaction.

EXPERIMENTAL PROCEDURES

Materials—α-Amylase was assayed colorimetrically using 0.3% and 0.1% soluble starch by the neocuproine method (*14*, *15*). Soluble starch (Lot M0R2968) as substrate and maltose as standard of the activity assay were purchased from Nacalai Tesque (Kyoto). Neocuproine-HCl (2,9-dimethyl-1,10-phenanthroline, Lot 21K1148) as coloring reagent B in the neocuproine method was obtained from Sigma (St. Louis, MO). Coloring reagent A (0.38 M Na_2CO_3, 1.8 mM $CuSO_4$, and 0.2 M glycine) in the neocuproine method was from Nacalai Tesque. All other chemicals were of reagent grade and purchased from Nacalai Tesque.

DNA Sequencing and Analysis—DNA sequence analysis was performed by the dideoxy chain termination method (*16*) with the AutoRead sequencing kit (Pharmacia-LKB Biotechnology, Uppsala, Sweden). After sub-cloning fragments of appropriate sizes in M13mp18,19 or pUC18,19, both strands were sequenced with fluorescent dye-linked universal primer or, in some cases, with the aid of internally priming oligonucleotides using an automated laser fluorescent DNA sequencer (A.L.F. Sequencer; Pharmacia-LKB Biotechnology). Insert-containing plasmid vectors used for double stranded-sequencing were purified on a CsCl/ethidium bromide gradient.

Mutagenesis—Exponentially growing cells of *B. licheniformis* IFO12196 strain in TYN broth at 50°C were harvested by centrifugation (5,000 × *g*, 10 min, 4°C) and suspended in LB broth containing 200 μg/ml NTG, and incubation was continued at 37°C for 30 min with gentle shaking. The cells were centrifuged (5,000 × *g*, 10 min, 4°C), washed three times with 50 mM Tris-HCl, pH 7.0, and then suspended in LB broth. Immediately the mutagenized cells were plated on LS plates (LB broth containing 6 g potato starch and 15 g agar per liter) to detect mutant strains. The cells generated an inner transparent and an outer turbid zone of starch hydrolysis around the colony.

Preparations of Enzymes—The wild-type α-amylase (PA) and mutant enzyme (MA) were purified by anion-exchange chromatography and dialysis according to the method previously reported (*13*). PA and MA were purified to homogeneity as judged by SDS-PAGE. The PA and MA concentrations were determined spectrophotometrically using the molar absorption coefficients (ε_{280}) of 1.348×10^5 and 1.409×10^5 M^{-1} cm^{-1}, and their molecular weights of 46,500 and 46,800, respectively (see "DISCUSSION").

Effect of Temperature on the Stability and Activity of α-Amylase—Effect of temperature on the stability of PA and MA was tested by measuring residual activity of starch hydrolysis after 1 h of incubation at 50–90°C, followed by cooling for 5 min on ice. Detailed procedures are described below.

1. Effect of 90°C on the stability at pH 6.0: 200 μl of 1 μM enzyme was added to 1,800 μl of pre-heated buffer at 90°C. The pre-heated buffers used were as follows: 20 mM acetate buffer (pH 4–5), 20 mM malate buffer (pH 5–6), 20 mM Tris-HCl (pH 7 and 8), 20 mM borate buffer (pH 9 and 10), and 20 mM bicarbonate buffer. After 1 h of incubation at 90°C, 200 μl of the solution was removed and cooled on ice for 5 min. Starch hydrolysis by the heat-treated enzyme was performed in 20 mM malate buffer, pH 6.0 (standard buffer) at 30°C for 3 min.

2. Effect of 95°C on the activity at pH 4–10: starch was hydrolyzed by PA and MA for 10 min at 95°C in the following buffers: 20 mM acetate buffer (pH 4.0, 4.5, and 5.0), 20 mM malate buffer (pH 5.0 and 6.0), 20 mM Tris-HCl buffer (pH 7.0 and 8.0), and 20 mM borate buffer (pH 9.0 and 10.0). Each buffer contained 5 mM $CaCl_2$, and the pH was adjusted to the respective values at 30°C.

3. Effect of temperature (80, 85, and 90°C) on the kinetic parameters of the thermal denaturation of PA and MA at various pH (pH 4.0, 5.0, 6.0, and 7.0): 100 μl of 10 μM enzyme in the buffers described above was mixed with 1.9 ml of the same buffer pre-heated at the temperature for thermal denaturation. At 1, 2, 3, 4, 5, 10, 15, 30, 45, and 60 min, 100 μl of the mixture was removed and added to 400 μl of the same buffer pre-cooled, then placed on ice for 5 min. The residual activity of starch hydrolysis was determined by mixing 100 μl of the heat-treated enzyme (100 nM) with 1.9 ml of substrate (3.0 mg/ml) in the standard buffer (pH 6.0) at 30°C and measuring the reaction product for 3 min. The initial concentrations of the enzyme and substrate were 5.0 nM and 2.85 g/ml, respectively. The apparent first-order rate constant (k) of the thermal inactivation was evaluated by plotting logarithmic values of the residual α-amylase activity against the time of heat treatment. The activation energy (E_a) for the thermal inactivation of PA and MA was determined from an Arrhenius plot ($\ln k$ *vs.* $1/T$) according to Eq. 1, and the Gibbs free energy of activation ($\Delta G^{\ddagger}$), the enthalpy of activation ($\Delta H^{\ddagger}$), and the entropy of activation ($\Delta S^{\ddagger}$) were determined from an Eyring plot according to Eqs. 2 and 3 (*17*, *18*).

$$\ln k = -(E_a/R)(1/T) \quad (1)$$

$$\triangle G^{\ddagger} = -RT\left[\ln \frac{hk}{k_B T}\right] \quad (2)$$

$$\ln \frac{hk}{k_B T} = \frac{\triangle H^{\ddagger}}{RT} + \frac{\triangle S^{\ddagger}}{R} \quad (3)$$

where k_B, h, and R are the Boltzmann, Plank, and gas constants, respectively. T is temperature in the Kelvin unit.

Activity Assay—α-Amylase activity was evaluated by the rate of increase in the reducing ends produced by the hydrolysis of soluble starch by the enzyme. The number of reducing ends was measured by the neocuproine method and calibrated with maltose as the standard. The reaction was initiated by adding the enzyme solution (10–20 μl) into 5 ml of the substrate incubated at 30°C. The enzyme

concentration and buffers used for the activity assay were as follows: the PA concentration was 8 nM at pH 2.8–3.0; 4 nM at pH 3.1–3.4 and 8.8–9.2; 2 nM at pH 3.6 and 8.0–8.4; and 1 nM at pH 3.6–7.6. The MA concentration was 4 nM at pH 2.8–3.2 and 8.8; and 2 nM at pH 3.3–8.4. Soluble starch powder (150 or 300 mg) was solubilized in 50 ml of the buffers described below, and the solution was heated in boiling water until it became transparent. The substrate solution was removed from the boiling-water bath and returned to a water bath at 30°C. The substrate solution was diluted with the respective buffers described above to the concentration of starch used in the assay at the pH indicated: 0.6–6.0 mg/ml (for PA assay) and 0.3–3.0 mg/ml (for MA assay) at pH 2.8–3.6; and 0.3–3.0 mg/ml (PA) and 0.05–1.0 mg/ml (MA) at pH 3.6–9.2. The buffers used were as follows: 20 mM glycine-HCl buffer (pH 2.8–3.6), 20 mM acetate buffer (pH 3.6–5.2), 20 mM malate buffer (pH 5.2–6.0), 20 mM sodium phosphate buffer (pH 6.0–8.0), and 20 mM borate buffer (pH 8.0–9.2), at 30°C.

Samples of the reaction solution (100 μl) were taken every 30 s over 2.5 min and added to 300 μl of 0.1 N NaOH to stop the reaction. Then 500 μl each of neocuproine solutions A and B were mixed with the sample solution. The mixture was heated in boiling water for 8 min, then cooled in iced water for 6 min. It was then diluted 2 times with distilled water, and the absorbance at 450 nm was measured with a Shimadzu UV-240 spectrophotometer (Kyoto) against water. By comparing the reducing power of the sample with that of maltose, the initial velocity (v) of enzyme-catalyzed hydrolysis of starch was calculated. From the initial velocity, kinetic parameters [the molecular activity (k_{cat}), Michaelis constant (K_m), and specificity constant (k_{cat}/K_m)] were calculated using the Michaelis-Menten equation with Kaleida Graph ver. 3.5 (Synergy Software, Reading, PA). The pH-independent molecular activity $(k_{cat})_o$ (or intrinsic molecular activity) and the proton dissociation constants (K_{es1} and K_{es2}) of the catalytic groups of the enzyme bound with substrate were calculated from the pH-dependence of k_{cat} using Eq. 4 (*19*).

$$k_{cat} = (k_{cat})_o/\{1 + ([H^+]/K_{es1}) + (K_{es2}/[H^+])\} \quad (4)$$

The pH-independent specificity constant $(k_{cat}/K_m)_o$ (or intrinsic specificity constant) and the proton dissociation constants (K_{e1} and K_{e2}) of the enzyme in the free state were calculated from the pH-dependence of k_{cat}/K_m using Eq. 5 (*19*).

$$k_{cat}/K_m = (k_{cat}/K_m)_o/\{1 + ([H^+]/K_{e1}) + (K_{e2}/[H^+])\} \quad (5)$$

Here, $pK_{es1} = -\log K_{es1}$; $pK_{es2} = -\log K_{es2}$; $pK_{e1} = -\log K_{e1}$; $pK_{e2} = -\log K_{e2}$, and pK_{es1} and pK_{e1} are on the acidic side, and pK_{es2} and pK_{e2} are on the alkaline side of the bell-shaped pH-dependence curve of k_{cat} and k_{cat}/K_m, respectively.

Differential Scanning Calorimetry (DSC)—The thermal denaturation of α-amylase was observed with a DSC system (VP-DSC of MicroCal LLC, Northampton, MA) with a scan rate of +1 K/min. The DSC data were analyzed by Origin 5.0 software of MicroCal with an add-in program made by Dr. S. Kitamura of Osaka Prefectural University, on the basis of an algorithm developed by Dr. J. M. Sturtevant of Yale University (*20*, *21*). The DSC measurements were performed at the α-amylase concentration of 0.11–0.49 mg/ml (2.4–10.5 μM) in 20 mM malate buffer (pH 6.0) and acetate buffer (pH 4.5), in the presence and absence of 5 mM $CaCl_2$.

RESULTS

DNA Sequencing of the α-Amylase Genes of B. licheniformis Strains—Eight amino acid residues of PA (*8*, *22*) were changed in MA: histidines at positions 133, 156, 293, and 450 were changed to tyrosines; glycines at 310 and 474 to aspartic acids; and alanines at 181 and 209 to Tyr and Val, respectively (Fig. 1).

Stability of PA and MA at High Temperature—PA and MA were treated at 90°C for 1 h at pH ranging from 4.0 to 11.0, and then the residual activity was measured in the standard buffer (pH 6.0) at 30°C. The heat stability of the enzymes at the pH examined was evaluated from the residual activity (Fig. 2). The activity for each enzyme (530 ± 45 and 420 ± 40 nM s^{-1} for PA and MA, respectively) obtained at pH 6.0 and 30°C before the heat treatment (here termed the intact activity) was set to 100% of the relative residual activity. It is interesting to note that the mutation of PA to MA hardly influenced the activity, and the intact activity of PA was only decreased to 80% by the mutation. MA showed higher residual activity than PA in the pH range examined, and preserved fully the intact activity even after the treatment at 90°C at pH 5.5–9.0 for 1 h. In contrast, when PA was treated at 90°C for 1 h at pH 6.0–7.0, the activity decreased to 80% of the intact activity. PA maintained 50% or more of the intact activity after the heat treatment at pH 5.5–10.0, and MA did so after the heat treatment at pH 5.0–10.5. It is noted that PA activity decreased to 50% after the heat treatment at pH 5.5, although MA activity was fully preserved after this treatment. Further, PA had no activity after the treatment at pH 5.0, but MA still remained 50%. MA kept 80% or more of the intact activity after the heat treatment in the pH range of 5.0–10.0, which is much wider than that (pH 6.0–7.0) of PA. These findings indicate that MA has higher heat stability at pH 5.0–10.6

```
ANLNGTLMQYFEWYMPNDGQHWKRLQNDSAYLAEHGITAVWIPPAYKGTS   50
QADVGYGAYDLYDLGEFHQKGTVRTKYGTKGELQSAIKSLHSRDINVYGD  100
VVINHKGGADATEDVTAVEVDPADRNRVISGEHLIKAWTHFHFPGRGSTY  150
                                  Y
SDFKWHWYHFDGTDWDESRKLNRIYKFQGKAWDWEVSNENGNYDYLMYAD  200
     Y                            Y
IDYDHPDVAAEIKRWGTWYANELQLDGFRLDAVKHIKFSFLRDWVNHVRE  250
        V
KTGKEMFTVAEYWQNDLGALENYLNKTNFNHSVFDVPLHYQFHAASTQGG  300
                                              Y
GYDMRKLLNGTVVSKHPLKSVTFVDNHDTQPGQSLESTVQTWFKPLAYAF  350
         D
ILTRESGYPQVFYGDMYGTKGDSQREIPALKHKIEPILKARKQYAYGAQH  400
DYFDHHDIVGWTREGDSSVANSGLAALITDGPGGAKRMYVGRQNAGETWH  450
                                                  Y
DITGNRSEPVVINSEGWGEFHVNGGSVSIYVQR   483
                        D
```

Fig. 1. **Primary structure of wild-type α -amylase (PA) from *Bacillus licheniformis* 1F019196.** The mutated sites of mutant α-amylase (MA) are underlined. Substitutions at the mutated amino acids are as follows: His (at positions 133, 156, 293, and 450) to Tyr; Gly (at 310 and 474) to Asp; Ala181 to Tyr; and Ala209 to Val.

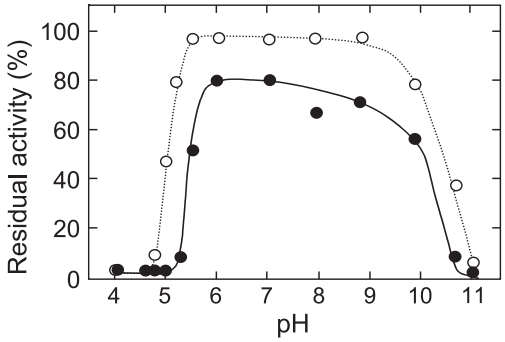

Fig. 2. **pH-dependency profiles of the stability of PA and MA after heat treatment.** The enzyme was incubated at 90°C for 1 h in the buffer at the indicated pH, and the residual activity of PA (solid circles) and MA (open circles) in starch hydrolysis was measured in 20 mM malate buffer, pH 6.0, and at 30°C. The respective activities of PA and MA at pH 6.0 and 30°C observed without heat treatment were 530 ± 45 and 420 ± 40 nM s^{-1}, and these values were set to 100% of their relative residual activities.

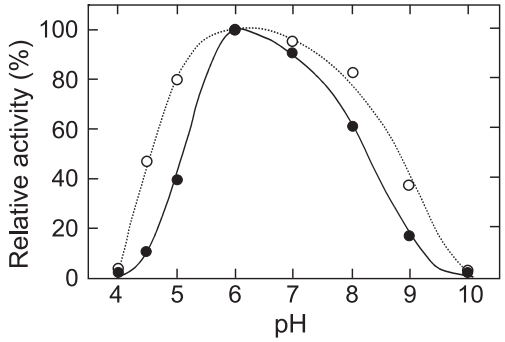

Fig. 3. **pH-dependency profiles of the activity of PA and MA at 95°C.** Starch hydrolysis activity of PA (solid circles) and MA (open circles) was measured at the indicated pH at 95°C for 10 min. The activities of PA and MA after heat treatment at pH 6.0 were 1.07 ± 0.15 and 1.66 ± 0.17 μM s^{-1}, respectively, and were set to 100% of the relative residual activities, respectively.

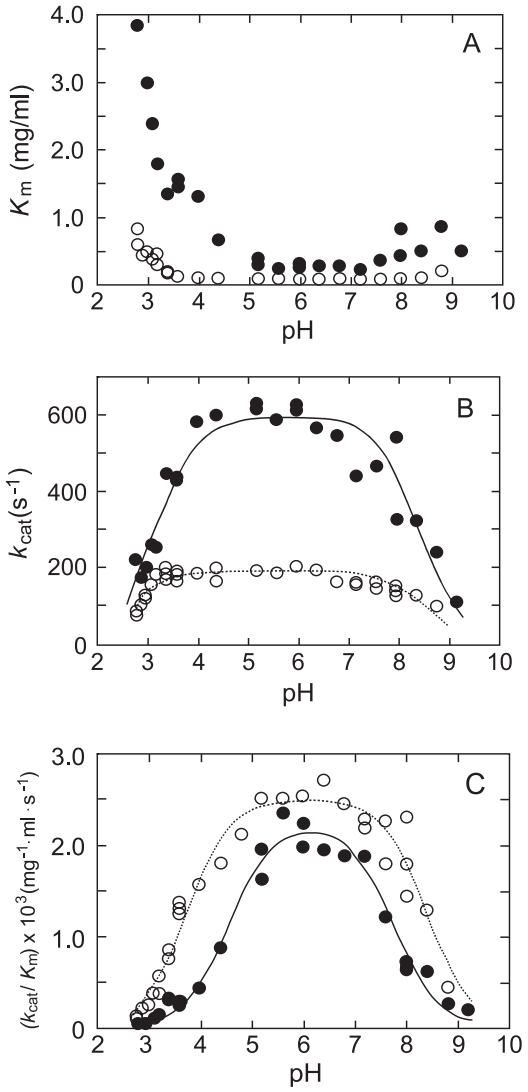

Fig. 4. **pH-dependency profiles of the kinetic parameters for starch hydrolysis activity of PA and MA.** The reactions were performed at the indicated pH and at 30°C. The relationship between the reaction rate (v) and the substrate concentration was analyzed by Hanes-Woolf plots ([S]/v *vs.* [S]) to evaluate the Michaelis constant (K_m), molecular activity (k_{cat}), and specificity constant (k_{cat}/K_m). Panels A, B, and C show the profiles for K_m, k_{cat}, and k_{cat}/K_m, respectively, in the hydrolysis with PA (solid circles) and MA (open circles).

than PA, and that MA retains considerable activity after heat treatment at pH 5.0–5.5, although PA destabilizes drastically at this pH.

Activity of PA and MA at High Temperature—Starch hydrolysis by PA and MA was performed at 95°C for 10 min at pH ranging from 4.0 to 10.0. The activity was evaluated from the amount of the reducing ends in a 10-min reaction, and the relative activity was plotted against pH (Fig. 3). The activities (1.07 ± 0.15 and 1.66 ± 0.18 μM s^{-1}, respectively) of PA and MA evaluated in the starch hydrolysis at 95°C for 10 min at pH 6.0 (optimal pH) were taken as 100% relative activity. It was shown that both enzymes have an optimal pH of 6.0 for starch hydrolysis at 95°C. In contrast to that at pH 6.0 and 30°C, the activity of MA at 95°C and pH 6.0 was higher than PA. MA showed higher relative activity than PA in the pH range examined, and MA was twice as active as PA at pH 5.0. The pH range where 50% or more of the maximal activity is maintained was wider for MA (pH 4.5–8.9) than PA (pH 5.1–8.2).

Effect of pH on the Starch Hydrolysis Catalyzed by PA and MA—The k_{cat} and k_{cat}/K_m values of PA and MA showed bell-shaped pH dependence at pH 2.8–9.2 and at 30°C (Fig. 4, B and C), indicating that the enzyme activities expressed by k_{cat} and k_{cat}/K_m are controlled by at least two ionizing functional groups (*17*, *19*, *23*). The acidic and alkaline pK_a values of the functional groups (pK_{e1}, and pK_{e2}) for the free PA enzyme were determined to be 4.47 ± 0.07 and 7.88 ± 0.06, and those for PA bound with substrate (pK_{es1}, and pK_{es2}) were 3.14 ± 0.07 and 8.09 ± 0.08, respectively. The pK_{e1} and pK_{e2} of MA were determined to be 3.71 ± 0.07 and 8.44 ± 0.09, and pK_{es1} and pK_{es2} to be 2.62 ± 0.09 and 8.56 ± 0.10, respectively. The acidic pK_a values (pK_{e1} = 3.71 ± 0.07 and pK_{es1} = 2.62 ± 0.09) of MA are significantly smaller than the respective values (pK_{e1} = 4.47 ± 0.07 and pK_{es1} = 3.14 ± 0.07) of PA, and the

alkaline pK_a values (pK_{e2} = 8.44 ± 0.09 and pK_{es2} = 8.56 ± 0.10) are larger than those (pK_{e2} = 7.88 ± 0.06 and pK_{es2} = 8.09 ± 0.08) of PA. Consequently, the active pH range is wider in MA than PA. The improved activity of MA under acidic and alkaline conditions (pH 3.5–5.5 and 7.0–8.5) may be derived from enhancement of catalytic efficiency and/or stability.

The K_m of MA was constant in the pH range of pH 3.5–8.5, and increased slightly at acidic pH lower than 3.5 and alkaline pH higher than 8.5 (Fig. 4A). On the other hand, the K_m of PA was constant at pH 5.0–7.0 and increased greatly with decreasing pH from 5.0 to 2.8 and slightly with increasing pH from 7.5 to 9.2. The K_m of MA was one-third of that of PA in the pH range of 5.0–7.0. Thus, MA has stronger affinity than PA to the starch substrate in the pH range examined. In particular, the affinity of PA decreases drastically at acidic pH lower than 4.5, while MA retains appreciable affinity in this pH range. It is suggested that the mutation of PA to MA enhances the affinity of the enzyme to the starch substrate.

The $(k_{cat})_o$ values of PA and MA were determined to be 595 ± 52 and 185 ± 17 s^{-1}, respectively, and the $(k_{cat}/K_m)_o$ values were 2,237 ± 110 and 2,537 ± 114 $mg^{-1}\cdot ml\cdot s^{-1}$. The $(k_{cat}/K_m)_o$ values of both enzymes were almost identical, while the $(k_{cat})_o$ and $(K_m)_o$ values of MA were one-third of those of PA. It is of interest to note that the mutation of PA to MA decreases the intrinsic activity $(k_{cat})_o$ to one-third, but increases the affinity $(1/K_m)$ to the substrate three times, and thus the intrinsic specificity constant $(k_{cat}/K_m)_o$ is not much changed.

Thermodynamic Parameters of Thermal Inactivation of PA and MA—The thermal inactivation of PA and MA was examined by incubating the enzyme at the concentration of 500 nM at pH 4.0, 5.0, 6.0 and 7.0 and a temperature of 50–90°C. Residual activity was measured at pH 6.0 and 30°C after the heat treatment. The initial concentrations of the enzyme and substrate were 5.0 nM and 2.85 mg/ml, respectively. The thermal inactivation was analyzed by assuming that it follows first-order kinetics, and the first-order rate constant (k) of the thermal inactivation was determined by plotting (ln [residual activity]) against time. The activation energy (E_a) of thermal inactivation was calculated from Arrhenius plots, and the thermodynamic parameters ($\Delta G^{\ddagger}$, $\Delta H^{\ddagger}$, and $\Delta S^{\ddagger}$) of activation for thermal inactivation were calculated from Eyring plots. Time-dependence curves of the residual activity of MA at pH 6.0 at 85, 90, and 95°C are shown in Fig. 5, A and B. The enzyme activity was not decreased at all by incubation at 85 and 90°C for 1 h, but decreased to 40% and 20%, respectively, after 50 h of incubation. On the other hand, the activity was decreased to 30% by incubation at 95°C for 1 h. It is obvious that the inactivation process shows two phases: a rapid first phase lasting up to 60 min (Fig. 5A), and a slower second phase from 1 to 50 h (Fig. 5B). The two-phase inactivation was less evident at the higher temperature, and the second phase almost disappeared in the inactivation at 95°C. The apparent first-order rate constants (k) of the thermal inactivation at 85, 90, and 95°C were determined to be 2.5 ± 0.3, 4.0 ± 0.5, and 163 ± 2 s^{-1}, respectively, from the first phase observed in Fig. 5A. These values were applied to Arrhenius plots (Fig. 5C) and Eyring plots (Fig. 5D). The parameters calculated are listed in Table 1.

In the case of PA, $\Delta G^{\ddagger}$ is maximal at pH 6.0, but the values of the other parameters increase with increasing pH and show maxima at pH 7.0. In the case of MA, all parameters show maxima at pH 6.0. The $\Delta G^{\ddagger}$ values of thermal inactivation of PA and MA are positive (ranging from 44 to 85 kJ mol^{-1}) in the pH range examined, but the $\Delta H^{\ddagger}$ values are much larger than the $\Delta G^{\ddagger}$ values. In other words, the activation process of the thermal inactivation of both enzymes is an endo-ergonic and endothermic reaction. The large $\Delta H^{\ddagger}$ value (88–460 kJ mol^{-1}) is compensated by the considerably large value (16–382 kJ mol^{-1}) of entropy change, $T\ \Delta S^{\ddagger}$. It can be said that the process is slightly enthalpy-driven. The E_a values of MA are much larger than those of PA at pH 5.0 and 6.0, although the values of both enzymes are almost the same at pH 4.0 and 7.0, suggesting that the thermal stability of MA is higher than that of PA at pH 5.0 and 6.0, but similar to that of PA at pH 4.0 and 7.0. This indicates that the mutation of PA to MA is effective in enhancing the thermal stability of BLA.

DSC Analysis—DSC measurements of PA and MA were performed at pH 4.5 and 6.0, in the presence and absence of 5 mM $CaCl_2$ (Fig. 6). As precipitates were formed during the heat treatment under the experimental conditions used, reversibility of the denaturation was not examined. A DSC curve (thermal capacity C_p *vs.* temperature) was observed, and the temperature T_{50}, at which a half of the protein is denatured, was determined from the temperature giving the highest value of the thermal capacity C_p. The denaturation enthalpy Δh_{cal} (J/g) was obtained from the peak area. The molar denaturation enthalpy ΔH_{cal} (kJ/mole) was given by multiplying Δh_{cal} by a molecular weight of 46,500 for PA and 46,800 for MA (see "DISCUSSION"). The values of T_{50} and ΔH_{cal} as well as the temperature at which the denaturation starts are listed in Table 2. The T_{50} values indicate that MA is more stable than PA in either the absence or presence of 5 mM $CaCl_2$. By the mutation of PA to MA, T_{50} increased by 9°C at pH 4.5 and 29°C at pH 6.0 in the absence of 5 mM $CaCl_2$; and by 22°C at both pH 4.5 and pH 6.0 in the presence of 5 mM $CaCl_2$. This suggests that the effect of the mutation of PA to MA on stabilizing the BLA enzyme is more obvious in the less stable enzyme at pH 4.5 than the more stable one at pH 6.0. Stabilization of the enzyme by Ca^{2+} ion is also more effective on the less stable enzyme (PA) than the more stable one (MA). The maximal stability was realized with MA at the optimal pH in the presence of Ca^{2+}.

DISCUSSION

Molecular Mass of BLA—The molecular masses of PA and MA evaluated by SDS-PAGE were reported to be 59 kDa and 61 kDa, respectively (*13*), and we also obtained the value of 55 kDa for both enzymes by SDS-PAGE. On the other hand, the molecular masses for PA and MA calculated from the amino acid compositions deduced from the nucleotide sequences are 46.5 and 46.8 kDa, respectively. Because we have confirmed that the enzymes contain no carbohydrates, these values of their molecular masses may be reasonable. The cause of this large discrepancy in the molecular masses is unclear. It is known that an average of 1.4 g of SDS binds to 1.0 g of protein denatured by SDS (*24*). When protein is resistant to SDS-denaturation, the

amount of SDS bound to the protein (1.0 g) might be less than the average value, and thus the mobility might be suppressed. Both PA and MA are highly thermostable, and resistance to SDS-denaturation is plausible. In this study, we used the molecular masses for PA and MA of 46.5 and 46.8 kDa, respectively. The molar absorption coefficients at 280 nm (ε_{280}) of PA and MA were calculated from the contents of Trp and Tyr residues using their respective ε_{280} values of 5,230 and 1,530 M^{-1} cm^{-1}. PA contains 17 Trp and 30 Tyr residues, and MA contains 17 Trp and 34 Tyr residues, and consequently the ε_{280} values of PA and MA were calculated to be 13.48×10^4 and 14.09×10^4 M^{-1} cm^{-1}, respectively; and thus the absorption coefficient A_{280} (10 mg/ml) values are 28.8 and 30.2.

Relationship between Amino Acid Substitution and the Activity—Eight amino acid residues of PA were substituted by the random mutation of PA to MA (Fig. 1). Negative charges of the protein are increased by the substitution of Tyr for His and of Asp for Gly, polarity is increased by the substitution of Tyr for Ala, and hydrophobicity is increased by the substitution of Val for Ala. However, no substitutions were observed in the case of active site residues (Asp231, Glu261, and Asp328), highly-preserved residues among α-amylases in the vicinity of the active site (Try56, Asp100, Val102, Lys234, Val259, Trp263, and His327), residues interacting with Ca ions (Asn104, Asp200, and His235) or residues interacting with Cl ions (Arg229, Asn326, and Gln300). Residues identified to interact intramolecularly with other residues (*8*) were also not substituted.

Although *Bacillus* α-amylases from thermophilic and mesophilic strains are quite different in thermal stability, they catalyze the same reaction with an identical mechanism, show similar three-dimensional structure, and have appreciably high amino acid sequence homology (*25*). Some general strategies for increasing the thermal stability of proteins have been proposed: strengthening hydrophobic interaction in intramolecular regions of proteins; introduction of hydrogen bonds and salt bridges; strengthening the secondary structure; introduction of metal ions such as Ca^{2+}; decreasing entropy in the denatured state by S-S bond and Pro substitution; and removing the denaturing factors. These strategies are effective in stabilization of human lysozyme (*26*, *27*). Similar strategy was applied to BLA, and the effect on the thermal stability of BLA of site-directed mutagenesis of His133 to Tyr (H133Y) and of Ala209 to Val (A209V) was reported (*28*). Interestingly,

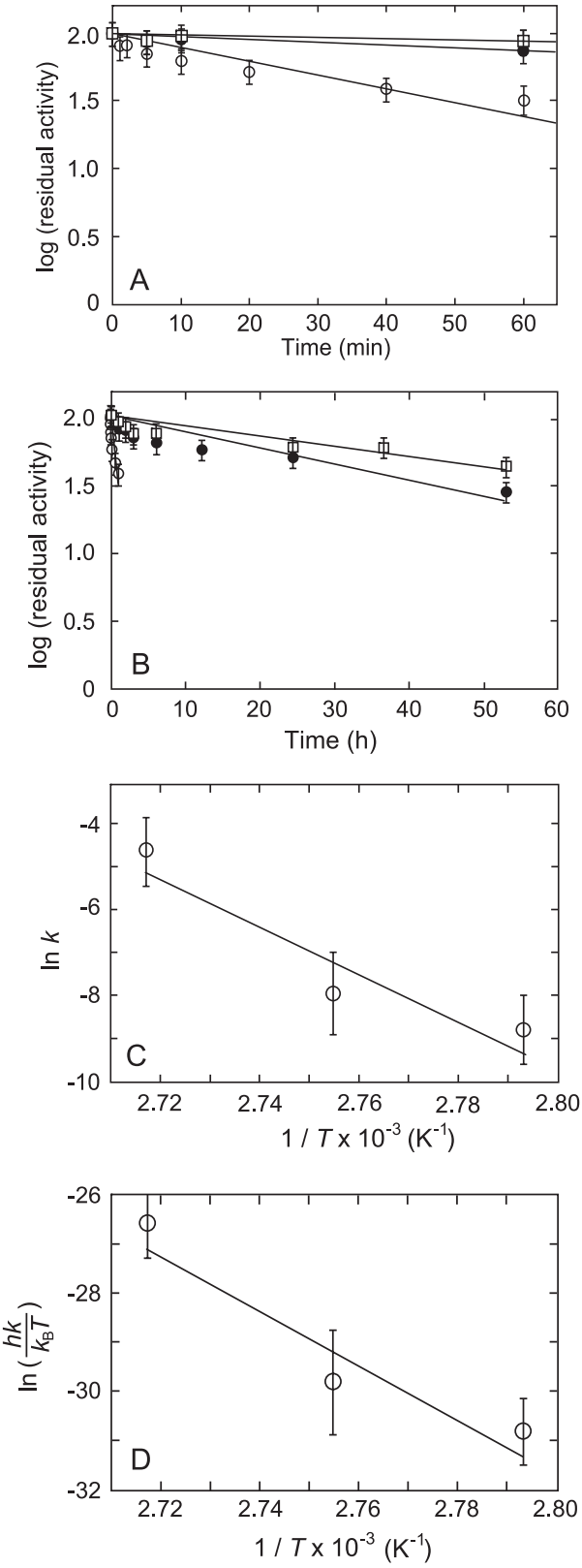

Fig. 5. **Thermal inactivation of MA.** Panels A and B: Time-dependence of the thermal inactivation of MA. MA at the concentration of 500 nM was incubated at 85°C (open squares), 90°C (solid circles), 95°C (open circles), in 20 mM malate buffer (pH 6.0) containing 5 mM $CaCl_2$ for the time indicated. The enzyme activity was measured in the standard buffer (pH 6.0) at 30°C, and the initial concentrations of MA and the substrate were 5 nM and 2.85 mg/ml, respectively. The first-order rate constants (k) for the thermal inactivation at 85, 90, and 95°C were determined to be $(2.5 \pm 0.3) \times 10^{-6}$, $(4.0 \times 0.5) \times 10^{-6}$, and $(16.3 \pm 0.2) \times 10^{-5}$ s^{-1}, respectively, from the inactivation progress observed in phase 1 shown in panel A. Using these values, the theoretical lines (solid lines) in panels A and B were drawn. The temperature (T_{50}) at which 50% of MA activity is lost in 30 min of incubation was determined to be 85°C. Panel C: Arrhenius plots of k. The activation energy of the thermal inactivation at pH 6.0 was determined to be (460 ± 208) kJ mol^{-1}. Panel D: Eyring plots of k. h and k_B are Planck constant and Boltzmann constant, respectively. The enthalpy ($\Delta H^{\ddagger}$) and entropy ($T\Delta S^{\ddagger}$) of activation at pH 6.0 were determined to be (460 ± 210) kJ mol^{-1} and (382 ± 210) J mol^{-1} K^{-1}, respectively.

Table 1. **Thermodynamic parameters for thermal inactivation of PA and MA at 90°C.**

	E_a (kJ/mol)	$\Delta G^{\ddagger}$ (kJ/mol)	$\Delta H^{\ddagger}$ (kJ/mol)	$T\Delta S^{\ddagger}$ (kJ/mol)
		PA		
pH 4.0	110 ± 11	48 ± 2	113 ± 11	65 ± 12
pH 5.0	158 ± 49	63 ± 3	161 ± 49	98 ± 51
pH 6.0	287 ± 49	65 ± 3	290 ± 49	225 ± 52
pH 7.0	339 ± 20	44 ± 1	42 ± 20	298 ± 21
		MA		
pH 4.0	85 ± 11	65 ± 3	88 ± 10	16 ± 10
pH 5.0	219 ± 10	77 ± 1	222 ± 10	145 ± 10
pH 6.0	460 ± 208	85 ± 5	460 ± 210	382 ± 210
pH 7.0	340 ± 10	69 ± 2	340 ± 10	271 ± 10

Table 2. **Thermodynamic parameters for the thermal inactivation of PA and MA as examined by DSC.**

BLA	PA				MA			
pH	pH 4.5		pH 6.0		pH 4.5		pH 6.0	
5 mM $CaCl_2$	−	+	−	+	−	+	−	+
T_s (°C)	31	52	57	74	40	66	84	100
T_{50} (°C)	41	63	71	84	50	85	100	106
Δh_{cal} (J/g)	2.6	2	0	4	5.6	26	66	35
ΔH_{cal} (kJ/mol)	156	720	1,800	2,640	336	1,560	3,960	2,100

T_s: temperature at which the denaturation starts; T_{50}: temperature at which a half of the protein is denatured; Δh_{cal} (J/g): denaturation enthalpy; ΔH_{cal} (kJ/mol): molar denaturation enthalpy.

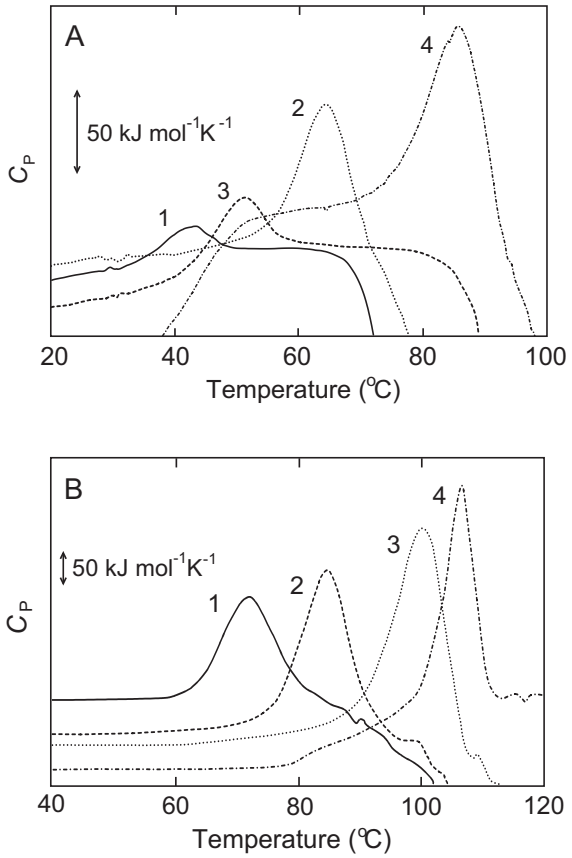

Fig. 6. **DSC curves of the thermal denaturation of PA and MA.** The measurements were done in 20 mM acetate buffer (pH 4.5; Panel A) and in 20 mM malate buffer (pH 6.0; Panel B), respectively, in the absence (curves 1 and 3) or presence (curves 2 and 4) of 5 mM $CaCl_2$. PA: curves 1 and 2; and MA: curves 3 and 4. Enzyme concentrations: [PA] = 0.49 mg/ml at pH 4.5 and at 0 M $CaCl_2$ (Panel A, curve 1); [PA] = 0.22 mg/ml at pH 4.5 and at 5 mM $CaCl_2$ (A, 2); [MA] = 0.40 mg/ml at pH 4.5 and at 0 M $CaCl_2$ (A, 3); pH 4.5 and at 5 mM $CaCl_2$ (A, 4); [PA] = 0.11 mg/ml at pH 6.0 and at 0 M $CaCl_2$ (B, 1); [PA] = 0.15 mg/ml at pH 6.0 and at 5 mM $CaCl_2$ (B, 2); [MA] = 0.16 mg/ml at pH 6.0 and at 0 M $CaCl_2$ (B, 3); [MA] = 0.15 mg/ml at pH 6.0 and at 5 mM $CaCl_2$ (B, 4).

these mutations were found in an MA enzyme produced by a *B. licheniformis* mutant obtained by random mutation of the wild-type strain (PA producer) and by screening temperature-resistant mutants. Thermal stability of the enzymes with a single mutation (H133Y or A209V) was increased, and that with double mutation (H133Y/A206V) was increased further. His133 is located at the surface of domain B and is the first residue of β-strand Bβ6, which is involved in forming a large central β-sheet in this domain (*8*). His133 contributes in forming hydrogen-bonding network with water and residues in β-sheets in domain B (Bβ4, Bβ5, and Bβ6). Substitution of a hydrophobic residue for His133 increases the thermal stability. The effect of the substitution of various residues was also reported (*29*). Ala209 is located close to the N-terminus of α-helix Aα3 in domain A (*8*, *25*), and forms a shallow indentation around the C_β atom. Substitution of a small hydrophobic residue for Ala209 increases the thermal stability. It is considered that the hydrophobic residue introduced at position 209 could contribute to the hydrophobic packing at the bottom of the indentation, resulting in an increase in the thermal stability of BLA protein. Two substitutions (H133Y and A209V) out of eight substitutions introduced into PA were considered to increase the thermal stability. The region between residues 178 and 199 forms a long loop comprising two extended segments that fill a large space between domains A and B. This loop contains three metal-binding residues and at least two residues implicated in substrate binding, and therefore its proper configuration could be crucial for the enzyme structure and function (*30*). Deletion of the loop region enhances the stability of various *Bacillus* amylases (*31*). Position 181 is included in this loop, and thus replacement of Ala181 with Tyr is considered to stabilize the overall structure of the enzyme by increasing hydrophobic interaction in the loop (*32*, *33*).

Increase in thermal stability of engineered proteins has often been reported to be accompanied with decrease in their catalytic activity at moderate temperature (*29*, *34–36*). Indeed, the starch hydrolysis activities of PA and MA are 530 ± 45 and 420 ± 40 nM s^{-1} respectively at pH 6.0 and 30°C (Fig. 2), while they are 1.07 ± 0.15 and 1.66 ± 0.17 μM s^{-1} respectively at pH 6.0 and 90°C (Fig. 3). The decrease in activity of MA compared to PA at 30°C might be explained by this assumption. The evidence that PA activity is lower than MA activity at 90°C might be due to the lower stability of PA than MA.

Site-directed mutagenesis of BLA has been performed by Declerck *et al*. (*36*). They reported that substitutions of Tyr for His156 and Ala181 improve the performance of BLA in industrial processes when combined with other stabilizing mutation (*36*). In the case of position

450 (His450), however, no significant thermal stabilization was observed (*30*). This position is located at the surface of domain C, which forms a distinct globular unit, although no distinct function could be ascribed to this domain with certainty. In the present study, we could not evaluate separately the effect of two substitutions at position 450 and 474. The effect of the substitutions at 293 and 310 were not discussed (*36*), although they are located in domain A. Interactions of these four residues with neighboring residues or metal ions have not yet been reported (*8*, *30*). However, the possibility that they are a factor for increasing the thermal stability of BLA cannot be excluded. Three-dimensional structure of the mutant enzyme might provide insights into the role of these residues. Further studies of these residues are required. Recently, we have isolated variants of *Bacillus amyloliquefaciens* α-amylase (BAA) with different thermal stability than the wild-type enzyme (*37*). It is known that BLA has a highly conserved similarity in structure and reaction mechanism. The BAA variants could be suitable models for designing BLA variants with improved thermal stability.

It is noteworthy that the amino acid substitution of PA influenced the catalytic properties as well as the thermal stability (Fig. 4). The K_m and k_{cat} of MA are one-third of those of PA in the pH range of 5.0–7.0, suggesting that the stability of the enzyme-substrate (ES) complex or the binding affinity of the enzyme with substrate is three times higher in MA than PA, while that of the transition state (TS) complex is three times higher in PA than MA. The improved affinity of MA for substrate seems to be gained at the expense of the destabilization of the TS complex. Consequently, PA and MA have almost the same value of the specificity constant k_{cat}/K_m. The stabilization effect for the ES and TS complexes is not high enough to identify the contribution of specific interactions. The amino acid substitution examined in this study could be a suitable clue for exploring the stabilizing factors for the ES and TS complexes of the *Bacillus* α-amylase.

This study was supported in part by Grants-in-Aid for Scientific Research (Nos. 14658203 and 17380065) from the Japan Society for the Promotion of Sciences, and grants (Nos. 0150 and 0345) from the Salt Science Foundation, Tokyo, Japan.

REFERENCES

1. Kuriki, T. and Imanaka, T. (1999) The concept of the α-amylase family: Structural similarity and common catalytic mechanism. *J. Biosci. Bioeng.* **87**, 557–565
2. Svensson, B. (1994) Protein engineering in the α-amylase family: catalytic mechanism, substrate specificity, and stability. *Plant. Mol. Biol*. **25**, 141–157
3. Janecek, S., Svensson, B., and Henrissat, B. (1997) Domain evolution in the α-amylase family. *J. Mol. Evol*. **45**, 322–331
4. MacGregor, E.A., Janecek, S., and Svensson, B. (2001) Relationship of sequence and structure to specificity in the α-amylase family of enzyme. *Biochem. Biophys. Acta* **1546**, 1–20
5. McCarter, J.D. and Withers, S.G. (1994) Mechanism of enzymatic glycoside hydrolysis. *Curr. Opin. Struct. Biol.* **4**, 885–892
6. McCarter, J.D. and Withers, S.G. (1996) Unequevocal identification of Asp-214 as the catalytic nucleophile of *Sacchalomyces cerevisiae* α-glucosidase using 5-fluoro glycosyl fluorides. *J. Biol. Chem.* **271**, 6889–6894
7. Nielson, J.E., Torben, V.B., and Gerrit, V. (2001) The determinant of α-amylase pH-activity profiles. *Protein Eng.* **14**, 505–512
8. Machius, M., Wiegand, G., and Huber, R. (1995) Crystal structure of calcium-depleted *Bacillus licheniformis* α-amylase at 2.2 Å resolution. *J. Mol. Biol.* **246**, 545–559
9. Nielson, J.E. and Torben, V.B. (2000) Protein engineering of bacterial α-amylases. *Biochem. Biophys. Acta* **1543**, 253–274
10. Crabb, W.D. and Mitchinson, C. (1997) Enzymes involved in the processing of starch to sugars. *Trends. Biotechnol.* **15**. 349–352
11. Andrew, S., Richard, B., and Anthony, G.D. (1999) Protein engineering of α-amylase for low pH performance. *Curr. Opin. Biotechnol.* 10, 349–352
12. Richardson, T.H., Tan, X., Frey, G. Callen, W., Cabell, M. Lam, D., Macomber, J., Short, J.M., Robertson, D.E., and Miller, C. (2002) A novel, high performance enzyme for starch liquefaction. *J. Biol. Chem.* **277**. 26501–26507
13. Endo, S. (1988) Thermostable bacterial α-amylases. in *Handbook of Amylases and Related Enzymes* (The Amylase Research Society of Japan, ed.) pp. 45–48, Pergamon Press, Oxford, U.K.
14. Brown, M.E. and Boston M.S. (1961) Ultra-micro sugar determinations using 2,9-dimethyl-1,10-phenanthroline hydrochloride (neocuproine). *Diabetes* **10**, 60–63
15. Warren, L.B. and Adrian, P. (1991) Estimation of cellulose activity using a glucose-oxidase-Cu(II) reducing assay for glucose. *J. Biochem. Biophys. Methods* **23**, 265–273
16. F. Sanger, S. Nicklen, and A.R. Coulson (1977) DNA sequencing with chain terminating inhibitors. *Proc. Natl. Acad. Sci. USA* **74**, 5463–5467
17. Segel, I.H. (1975) *Enzyme Kinetics*, pp. 926–942, John Wiley and Sons, New York
18. Oneda, H., Lee, S., and Inouye, K. (2004) Inhibitory effect of 0.19 α-amylase inhibitor from wheat kernel on the activity of porcine pancreas α-amylase and its thermal stability. *J. Biochem.* **135**, 421–427
19. Hiromi, K. Takahashi, K. Hamauzu, Z., and Ono, S. (1966) Kinetics studies on glucoamylase. *J. Biochem.* **59**, 469–475
20. Kitamura, S. and Sturtevant, J.M. (1989) A scanning calorimetric study of the thermal denaturation of the lysozyme of phage T4 and the Arg96→His mutant thereof. *Biochemistry* **28**, 3788–3792
21. Tanaka, A., Okuda, K., Senoo, K., Obata, H., and Inouye, K. (1999) Guanidine hydrochloride-induced denaturation of *Pseudomonas cepacia* lipase. *J. Biochem.* **126**, 382–386
22. Yuuki, T., Nomura, T., Tezuka, H., Tsuboi, H., Yamagata, H., Tsukagoshi, N., and Udaka, S. (1985) Complete nucleotide sequence of a gene coding for heat- and pH-stable a-amylase of *Bacillus licheniformis*: Comparison of the amino acid sequence of three bacterial liquefying α-amylases deduced from the DNA sequences. *J. Biochem.* **98**, 1147–1156
23. Muta, Y. Oneda, H., and Inouye, K. (2005) Anomalous pH-dependence of the activity of human matrilysin (matrix metalloproteinase-7) as revealed by nitration and amination of its tyrosine residues. *Biochem. J.* **386**, 263–270
24. Inouye, K., Tonomura, B., and Hiromi, K. (1979) The effec of sodium dodecyl sulfate on the structure and function of a protein proteinase inhibitor, *Streptomyces* subtilisin inhibitor. *Arch. Biochem. Biophys.* **192**, 260–269
25. Fitter, J., Herrmann, R., Dencher, N.A., Blume, A., and Hauss, T. (2001) Activity and stability of a thermastable α-amylase compared to its mesophilic homologue: mechanism of thermal adaptation. *Biochemistry* **40**, 10723–10731
26. Funahashi, J., Takano, K., Yamagata, Y., and Yutani, K. (2000) Role of surface hydrophobic residues in the conformational stability of human lysozyme at three different positions. *Biochemistry* **39**, 14448–14456

27. Takano, K., Yamagata, Y., and Yutani, K. (2001) Contribution of polar groups in the interior of a protein to the conformational stability. *Biochemistry* **40**, 4853–4858
28. Declerck, N., Machius, M., Chambert, R., Wiegand, G., Huber, R., and Gaillardin, C. (1997) Hyperthermostable mutants of *Bacillus licheniformis* α-amylase: thermodynamic studies and structural interpretation. *Protein Eng.* **10**, 541–549
29. Machius, M., Declerck, N., Huber, R., and Wiegand, G. (2003) Kinetic stabilization of *Bacillus licheniformis* α-amylase through introduction of hydrophobic residues at the surface. *J. Biol. Chem.* **267**, 11546–11553
30. Declerck, N., Machius, M., Wiegand, G., Huber, R., and Gaillardin, C. (2000) Probing structural determinants specifying high thermostability in *Bacillus licheniformis* α-amylase. *J. Mol. Biol.* **301**, 1041–1057
31. Igarashi, K., Hatada, Y., Ikawa, K., Araki, H., Ozawa, T., Kobayashi, T., Ozaki, K., and Ito, S. (1998) Improved thermostability of *Bacillus* α-amylase by deletion of an arginine-glycine residue is caused by enhancement calcium binding. *Biochem. Biophys. Res. Commun.* **248**, 372–377
32. Vielle, C. and Zeikus, G. (1996) Thermozyme: identifying molecular determinants of protein structural and functional stability. *Trends. Biotechnol.* **14**, 183–190
33. Jaenicke, R. and Böhm, G. (1998) The stability of proteins in extreme environments. *Curr. Opin. Struct. Biol.* **8**, 738–738
34. Suzuki, Y., Ito, N., Yuuki, T., Yamagata, H., and Udaka, S. (1989) Amino acid residues stabilizing a *Bacillus* α-amylase against irreversible thermoinactivation. *J. Biol. Chem.* **264**, 18933–18938
35. Declerck, N., Joyet, P., Gaillardin, C., and Masson, J.-M. (1990) Use of amber suppressor to investigate the thermostability of *Bacillus licheniformis* α-amylase. *J. Biol. Chem.* **265**, 15481–15488
36. Declerck, N., Machius, M., Joyet, P., Wiegand, G., Huber, R., and Gaillardin, C. (2003) Hyperthermostabilization of *Bacillus licheniformis* α-amylase and modulation of its stability over 50°C temperature range. *Protein Eng.* **16**, 287–293
37. Lee, S., Mouri, Y., Minoda, M., Oneda, H., and Inouye, K. (2006) Comparison of the wild-type α-amylase and its variant enzymes in *Bacillus amyloliquefaciens* in activity and thermal stability, and insights into engineering the thermal stability of *Bacillus* α-amylase. *J. Biochem.* **139**, 1007–1015